

Supporting Information

Bifurcation of Regeneration and Recombination in Dye-Sensitized Solar Cells via Electronic Manipulation of Tandem Cobalt Redox Shuttles

Josh Baillargeon, Yuling Xie and Thomas W. Hamann*

Department of Chemistry, Michigan State University, 578 S Shaw Lane, East Lansing, Michigan
48824-1322, United States.

*Email hamann@chemistry.msu.edu (T.W.H.).

Materials and Methods

Materials. All materials were purchased from commercial suppliers and used as received, with the exception of tetrahydrofuran (THF), acetonitrile and tetrabutylammonium hexafluorophosphate (TBAPF₆). The THF (Fisher Chemical, Optima) used in the synthesis of [Co(ptypy)₃], where ptypy represents 2-(p-Tolyl)pyridine, was distilled over sodium/benzophenone and stored in a glovebox (MBRAUN Labmaster SP) prior to use. Acetonitrile (Fisher Chemical Certified ACS, ≥ 99.5%), used in all electrochemistry, stopped-flow and solar cell measurements, was purified on an activated alumina column before being stored in a glovebox. TBAPF₆, (Sigma-Aldrich, 98%) was recrystallized from ethanol/diethyl ether and dried under vacuum. Both supporting electrolytes, TBAPF₆ and lithium bis(trifluoromethane)sulfonamide, LiTFSI, were stored in a glovebox under moisture free conditions prior to use.

Synthesis of Redox Shuttles. The synthesis of the [Co(bpy)₃](TFSI)₂ and [Co(bpy)₃](TFSI)₃ redox shuttles, where bpy represents 2,2'-bipyridine and TFSI is bis(trifluoromethane)sulfonidmide, were prepared as previously described.¹ The [Co(bpyCl₂)₃](PF₆)₂ complex, where bpyCl₂ is 4,4'-dichloro-2,2'-bipyridine and PF₆ is hexafluorophosphate, was also prepared using a previously published procedure.² However, oxidation to [Co(bpyCl₂)₃](PF₆)₃ was carried out using 1.2 equivalents of NOPF₆ in a minimal amount (~5 mL) of acetonitrile. The reaction mixture was allowed to stir for 30 minutes before being concentrated, precipitated with diethyl ether, vacuum filtered and washed with methanol, water and diethyl ether. The synthesis and purification of the [Co(ptypy)₃] complex was carried out using a modified procedure from the literature.³ Such changes included purchasing the 2-mesitylmagnesium bromide Grignard reagent (Sigma-Aldrich) prior to use rather than making it in-situ, as well as replacing the original ligand 2-phenylpyridine with 2-(p-Tolyl)pyridine. Both [Co(bpyCl₂)₃](PF₆)_{3/2} and [Co(ptypy)₃] were characterized using elemental analysis, Table S1. [Co(ptypy)₃] was further characterized using ¹H NMR. ¹H NMR (500 MHz, Chloroform-*d*) δ 7.79 (dt, *J* = 8.2, 1.1 Hz, 1H), 7.58 (ddd, *J* = 8.1, 7.3, 1.6 Hz, 1H), 7.53 (d, *J* = 7.8 Hz, 1H), 7.18 (ddd, *J* = 5.6, 1.7, 0.8 Hz, 1H), 6.77 (ddd, *J* = 7.1, 5.6, 1.3 Hz, 1H), 6.74 – 6.68 (m, 1H), 6.33 (d, *J* = 1.6 Hz, 1H), 2.08 (s, 3H).

Electrochemistry. Cyclic voltammetry (CV) measurements were performed with an Autolab PGSTAT 126N potentiostat using a platinum disk working electrode, platinum mesh counter electrode and Ag/AgNO₃ (0.1 M TBAPF₆ acetonitrile) reference electrode. The error associated

with each redox shuttle's formal potential, E° , is based on the standard deviation of the formal potentials measured over three separate days. Reference conversion to NHE was done assuming the potential of Ferrocene in acetonitrile is 0.40 V vs SCE.⁴ The active area of the platinum disk electrode was determined to be 0.024 cm² based on capacitance measurements using CV.

Cross-Exchange Kinetics. All stopped-flow measurements were performed using a similar methodology to that previously reported.⁵ Briefly, samples were measured using an Olis RSM 1000 DeSa rapid-scanning spectrophotometer with dual-beam UV-Vis recording to Olis SpectralWorks software. The instrument contained a quartz cell with a 2 cm path length. Scans were taken once every millisecond with 1 nm resolution. The 150 W Xenon arc lamp was controlled using an LPS-220B Lamp Power Supply and held to within 79-80 W during each measurement. The temperature was also held constant at $25 \pm 0.1^\circ\text{C}$ using a NESLAB RTE-140 chiller/circulator. All [Co(ppy)₃] and [Co(bpyCl₂)₃](PF₆)_{3/2} solutions were prepared using dry acetonitrile. The ionic strengths were adjusted to 0.1 M using TBAPF₆.

Pseudo-first order conditions were implemented, which maintained at least a 10-fold excess of a single reactant and product species. Both of the [Co(bpyCl₂)₃](PF₆)₃ and [Co(bpyCl₂)₃](PF₆)₂ concentrations for these measurements were held in excess while the [Co(bpyCl₂)₃](PF₆)₃ concentration was varied for the reactions with [Co(ppy)₃]. The spectral changes were monitored at 433 nm, following the decaying absorbance of the [Co(ppy)₃] species. Scientific Data Analysis Software provided fits for the pseudo-first order rate constants, k_{obs} , using a nonlinear least-squares regression. Seven independent trials were averaged to provide the measured k_{obs} values. Absorbance plots for each pseudo-first order reaction were fit using: $A = A_\infty + (A_0 - A_\infty)e^{-k_{\text{obs}}t}$. The second-order rate constants were calculated from the slope of the k_{obs} versus the concentration of excess [Co(bpyCl₂)₃](PF₆)₃, which had a goodness of fit, $R^2 > 0.999$. The error associated with measured k_{obs} values were taken to be the standard deviation of the seven independent trials. The minimal error in concentration was propagated based on prepared stock solutions of each reaction mixture.

Solar Cell Fabrication & Characterization. Solar cell fabrication and characterization was performed using a previously reported procedure as well.⁵ Briefly, fluorine-doped tin oxide (FTO) glass substrates (TEC 15, Hartford), 12 Ω cm⁻², were used to prepare the titanium dioxide (TiO₂) photoanodes. The glass substrates were cleaned in an ultrasonic bath using (in order) soap water,

deionized water, isopropyl alcohol and acetone. Atomic layer deposition (ALD) was used to provide a blocking layer of TiO₂. A Savannah 200 instrument (Cambridge Nanotech Inc) deposited 1000 cycles of titanium isopropoxide (99.999% trace metals basis, Sigma-Aldrich) at 225°C and water using reactant exposure times of 0.3 s and 0.015 s, respectively. Between each exposure, nitrogen was purged for 5 s. A transparent TiO₂ nanoparticle layer was prepared by doctor blading a paste of 15-20 nm TiO₂ nanoparticles (Ti-Nanoxide T/SP, Solaronix) on the TiO₂ coated FTO-glass substrate. The doctor bladed TiO₂ film was allowed to relax for 10 min at room temperature and 10 minutes at 100°C. The electrodes were then annealed by heating in air to 325°C for 5 min, 375°C for 5 min, 450°C for 5 min and 500°C for 15 min. The electrodes were allowed to cool to a temperature of 80°C before being immersed in a D35cpdt dye solution consisting of 0.2 mM D35cpdt (Dyename, 95%) and 5 mM chenodeoxycholic acid (Solaronix) in ethanol, and left to soak overnight in the dark. After 20-24 hours, the electrodes were rinsed with acetonitrile. A ~25 µm thick Surlyn frame (Solaronix) was sandwiched between the TiO₂ nanoparticle electrode and a platinized FTO electrode. Light pressure was applied at ~100°C to seal the cell. Electrolyte was introduced by capillary forces through two pre-drilled holes on the platinum counter electrode, which were subsequently sealed with microglass (VWR) and Surlyn film. Eight cells were prepared in total using two different electrolytes. The compositions of each electrolyte were as follows: 1) 0.2 M [Co(bpy)₃](TFSI)₂, 20 mM [Co(bpy)₃](TFSI)₃, and 0.1 M LiTFSI (Sigma-Aldrich, 99.95% trace metal basis) in acetonitrile. 2) 0.2 M [Co(bpy)₃](TFSI)₂, 20 mM [Co(bpy)₃](TFSI)₃, 0.61 mM [Co(ppy)₃] and 0.1 M LiTFSI in acetonitrile.

Photoelectrochemical measurements were performed with a potentiostat (Autolab PGSTAT 126N) interfaced with a Xenon Arc Lamp. An AM 1.5 solar filter was used to simulate sunlight at 100 mW cm⁻² and the light intensity was calibrated with a certified reference cell system (Oriel® Reference Solar Cell & Meter). An additional 400 nm longpass filter was used to prevent direct excitation of the TiO₂ in all light measurements. A black mask with an aperture area (0.4 × 0.4 cm²) was applied on top of the cell. A set of neutral density filters (Thorlabs NEK01S) was used to conduct light intensity dependence measurements. Open circuit voltage decay (OCVD) measurements were performed in two different ways. Both were measured under galvanostatic conditions; however, in order to determine the recombination associated with the [Co(ppy)₃]⁺, OCVD measurements for the tandem cells were measured under light and dark conditions. Dark

OCVD measurements were completed by applying the DSSCs open circuit potential for twenty seconds then measuring the cells open circuit voltage as it decayed back to solution potential.

Incident Photon to Current Efficiency (IPCE) measurements, performed under monochromatic light, were completed using a monochromator (Horiba Jobin Yvon MicroHR) attached to the 450 W Xenon arc light source. Both entrance and exit slit width were set to 0.75 mm to meet an 8 nm line width for good resolution IPCEs. The photon flux of the light incident on the samples was measured with a laser power meter (Nova II Ophir). IPCE measurements were made at 10 nm intervals between 400 nm and 750 nm at short circuit in the absence of bias light.

Table S1. Elemental analysis results.

Compound	Calculated			Found		
	C(%)	H(%)	N(%)	C(%)	H(%)	N(%)
[Co(bpyCl ₂) ₃](PF ₆) ₂ C ₃₀ H ₁₈ N ₆ CoCl ₆ P ₂ F ₁₂	35.2	1.8	8.2	34.8	1.6	8.1
[Co(bpyCl ₂) ₃](PF ₆) ₃ C ₃₀ H ₁₈ N ₆ CoCl ₆ P ₃ F ₁₈	30.8	1.6	7.2	30.1	1.2	7.2
[Co(ptypy) ₃] C ₃₆ H ₃₀ N ₃ Co	76.7	5.4	7.5	75.2	5.2	7.2

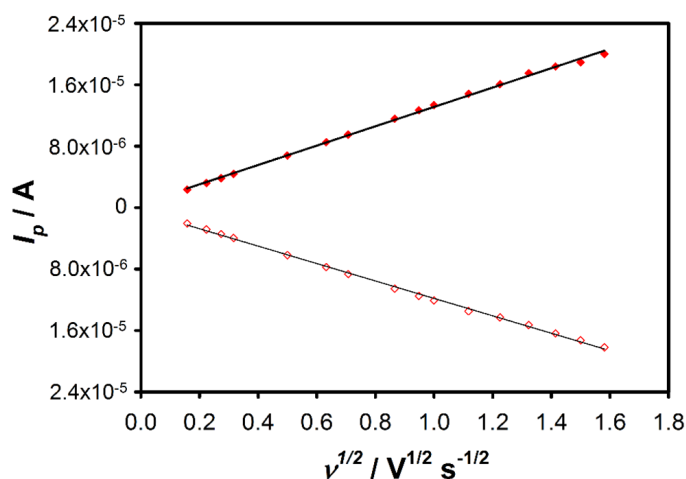


Figure S1. Randles-Sevcik plot of both anodic (filled red diamonds) and cathodic (open red diamonds) peak currents versus the square root of the scan rate for the [Co(ptypy)₃] scan rate dependence, Figure 1b.

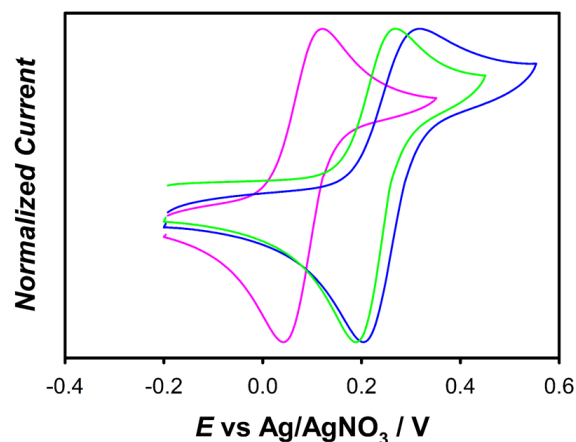


Figure S2. Normalized cyclic voltammograms of $[\text{Fe}(\text{C}_5\text{H}_5)_2]$ (pink), $[\text{Co}(\text{pty})_3]$ (green) and $[\text{Co}(\text{bpyCl}_2)_3](\text{PF}_6)_2$ (blue) in acetonitrile with 0.1 M TBAPF_6 supporting electrolyte at a scan rate of 100 mV/s using a platinum disk working electrode, platinum mesh counter electrode and Ag/AgNO_3 (0.1 M TBAPF_6 acetonitrile) reference electrode.

Table S2. Observed rate constants, k_{obs} , and the initial reaction mixtures for the cross-exchange between $[\text{Co}(\text{pty})_3]$ and $[\text{Co}(\text{bpyCl}_2)_3](\text{PF}_6)_3$.

$[\text{Co}(\text{pty})_3]/(\text{M})$	$[\text{Co}(\text{bpyCl}_2)_3]^{3+}/(\text{M})$	$[\text{Co}(\text{bpyCl}_2)_3]^{2+}/(\text{M})$	$k_{\text{obs}}/(\text{s}^{-1})$
5.00×10^{-5}	5.00×10^{-4}	5.00×10^{-4}	18.1 ± 0.2
	1.00×10^{-3}		33.1 ± 0.5
	1.50×10^{-3}		48.9 ± 0.7
	2.00×10^{-3}		64.6 ± 1.5
	2.74×10^{-3}		89.7 ± 2.6
	3.00×10^{-3}		95.0 ± 4.4

Cross Exchange Kinetics – Non-Linear Correction (f_{12}) & Work Term (W_{12}) Calculations:^{5,6}

As previously described, the non-linear correction parameter, f_{12} , was determined from equation S1, where T is the temperature, k_B is the Boltzmann constant and Z is the frequency factor. For this calculation it is assumed that Z is $10^{11} \text{ M}^{-1}\text{s}^{-1}$. The work terms associated with the electrostatic interactions of the forward and reverse cross-exchange reactions are also included and are represented by w_{12} and w_{21} , and by w_{11} and w_{22} for the self-exchange reactions.

$$\ln f_{12} = \frac{1}{4} \frac{\left(\ln K_{12} + \frac{w_{12} - w_{21}}{k_B T} \right)^2}{\ln \left(\frac{k_{11} k_{22}}{Z^2} \right) + \left(\frac{w_{11} + w_{22}}{k_B T} \right)} \quad (\text{S1})$$

The work associated with bringing the precursor complexes a separation distance, r , for electron transfer to occur was calculated using equations S2 and S3.

$$W_{12} = \exp \left[- \left(w_{12} + w_{21} - w_{11} - w_{22} \right) / 2RT \right] \quad (\text{S2})$$

$$w_{ij}(r) = \frac{z_i z_j q^2 N_A}{4\pi\epsilon_0 \epsilon r (1 + \beta r)} \quad (\text{S3})$$

Equation S3 was used to determine the work associated with the forward cross-exchange reaction, w_{12} , the reverse cross-exchange, w_{21} , and the self-exchanges of both reactants, w_{11} and w_{22} , respectively, for reaction 1. Here z_i and z_j are the charges of the reacting ions, q is the charge on an electron, N_A is Avogadro's constant, ϵ_0 is the permittivity of free space, ϵ is the static dielectric of the medium, $\beta = \left(2q^2 N_A I / 1000 \epsilon_0 \epsilon k_B T \right)^{1/2}$, I is the ionic strength of the solution and k_B is Boltzmann's constant. It is assumed in these calculations that the work is primarily Coulombic, the reactants are spherical, and the separation distance, r , is simply the center-to-center distance when the reactants come into contact. The work term, W_{12} , calculated for reaction 1, was determined to be 2.2; however, the calculated work is a crude approximation since the Debye-Huckel model is not expected to provide extremely accurate values at high ionic strengths, such as those used in these measurements.

Table S3. Kinetic summary of the cross-exchange rate constants, k_{12} and k_{21} , measured equilibrium constants for the forward reaction, K_{12} , the nonlinear correction term, f_{12} , and work term, W_{12} , associated with bringing precursor complexes together for reaction 1 between $[\text{Co}(\text{bpyCl}_2)_3](\text{PF}_6)_3$ and $[\text{Co}(\text{ptpy})_3]$ in acetonitrile with 0.1 M TBAPF₆ at $25 \pm 0.1^\circ\text{C}$.

Kinetic Parameter	Cross-exchange values
K_{12} (Nernst)	3.5 ± 1.3
K_{12} (k_{12} / k_{21})	7.7 ± 3.7

$k_{12} / (\text{M}^{-1}\text{s}^{-1})$	$(6.3 \pm 0.1) \times 10^4$
$k_{21} / (\text{M}^{-1}\text{s}^{-1})$	$(8.2 \pm 3.9) \times 10^3$
f_{12}	0.92
W_{12}	2.2

Table S4. Formal reduction potentials, E° , of all cobalt complexes used in stopped-flow and DSSC studies: cobalt tris(2-(p-tolyl)pyridine), $[\text{Co}(\text{ptpy})_3]^{+/0}$, cobalt tris(4,4'-dichloro-2,2'-bipyridine), $[\text{Co}(\text{bpyCl}_2)_3]^{3+/2+}$, and cobalt tris(2,2'-bipyridine), $[\text{Co}(\text{bpy})_3]^{3+/2+}$. Ferrocene, $[\text{Fe}(\text{C}_5\text{H}_5)_2]^{+/0}$, is also included as a point of reference in converting from Ag/AgNO₃ to NHE. All formal potentials were measured using in acetonitrile with 0.1 M TBAPF₆ or 0.1 M LiTFSI supporting electrolyte with a platinum working electrode, platinum mesh counter electrode and a Ag/AgNO₃ reference electrode (0.1 M TBAPF₆ acetonitrile).

Redox Couple	E° (mV vs Ag/AgNO ₃)
$[\text{Co}(\text{ptpy})_3]^{+/0}$	231 ± 9
$[\text{Co}(\text{bpyCl}_2)_3]^{3+/2+}$	263 ± 2
$[\text{Co}(\text{bpy})_3]^{3+/2+}$	29 ± 10
$[\text{Fe}(\text{C}_5\text{H}_5)_2]^{+/0}$	86 ± 10

Table S5. Average J - V Characteristics of four DSSCs containing a tandem electrolyte of $[\text{Co}(\text{ptpy})_3]$ and $[\text{Co}(\text{bpy})_3]^{3+/2+}$ and four with only $[\text{Co}(\text{bpy})_3]^{3+/2+}$ both paired with the D35cpdt dye under simulated AM 1.5G illumination (100 mW cm^{-2}).

Electrolyte	$[\text{Co}(\text{bpy})_3]^{3+/2+}$	$[\text{Co}(\text{ptpy})_3]$ & $[\text{Co}(\text{bpy})_3]^{3+/2+}$
η (%)	1.99 ± 0.11	2.37 ± 0.07
J_{sc} (mA cm ⁻²)	4.88 ± 0.17	5.74 ± 0.24
V_{oc} (V)	0.58 ± 0.01	0.60 ± 0.01
ff	0.70 ± 0.04	0.68 ± 0.04

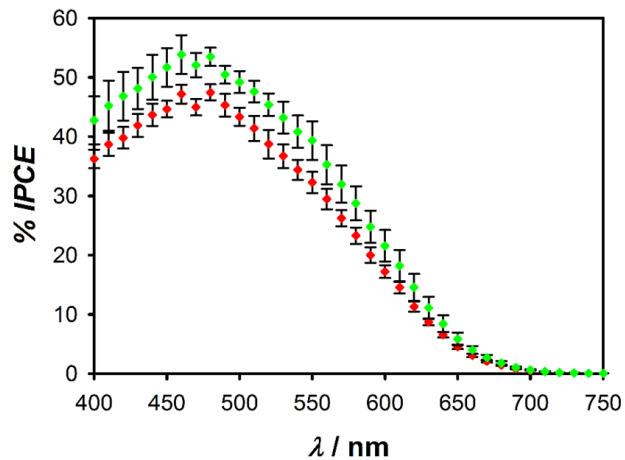


Figure S3. IPCE plots of DSSCs containing a $[\text{Co}(\text{bpy})_3]^{3+/2+}$ electrolyte (red dots) and a tandem electrolyte containing $[\text{Co}(\text{ptpy})_3]$ and $[\text{Co}(\text{bpy})_3]^{3+/2+}$ (green dots).

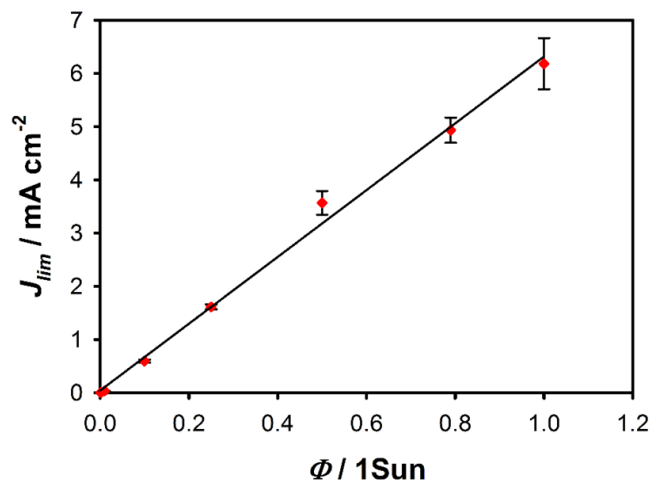


Figure S4. Light intensity dependence on short circuit photocurrent, J_{lim} , in DSSCs employing a tandem electrolyte of $[\text{Co}(\text{ptpy})_3]$ and $[\text{Co}(\text{bpy})_3]^{3+/2+}$.

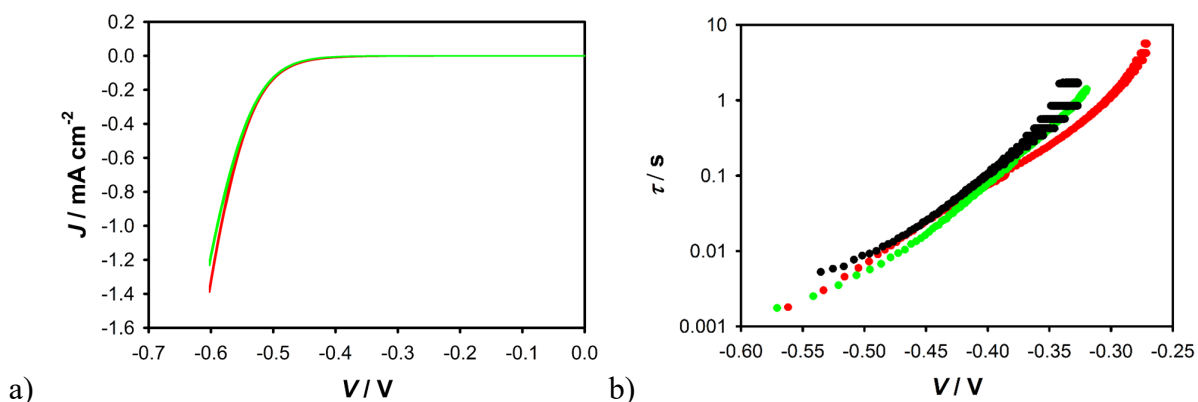


Figure S5. a) J - V curves corresponding to DSSCs filled with $[\text{Co}(\text{bpy})_3]^{3+/2+}$ electrolyte (red) and a tandem electrolyte containing $[\text{Co}(\text{ptpy})_3]$ & $[\text{Co}(\text{bpy})_3]^{3+/2+}$ (green) measured in the dark. b) Electron lifetimes of DSSCs containing a $[\text{Co}(\text{bpy})_3]^{3+/2+}$ electrolyte (red) and a tandem electrolyte containing $[\text{Co}(\text{ptpy})_3]$ & $[\text{Co}(\text{bpy})_3]^{3+/2+}$ (green) using open circuit voltage decay (OCVD). To make sure recombination to $[\text{Co}(\text{ptpy})_3]^+$ wasn't a major component under illumination, OCVD was employed in the dark to cells containing the tandem electrolyte (black). These measurements were achieved by applying the open circuit potential in the dark, whereupon the potential was released and allowed to equilibrate back to the solution potential under galvanostatic conditions.

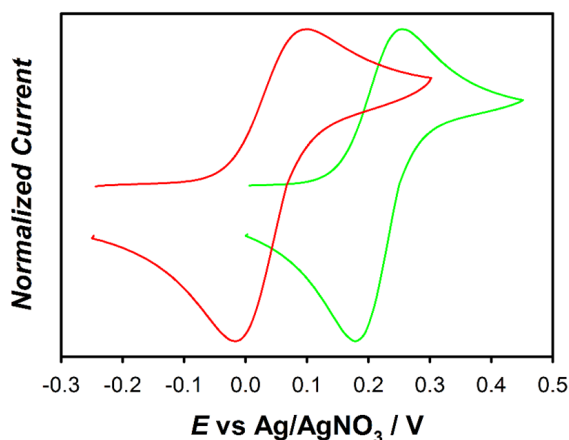


Figure S6. Normalized cyclic voltammograms of $[\text{Co}(\text{bpy})_3](\text{TFSI})_2$ (red) and $[\text{Co}(\text{ptpy})_3]$ (green) in acetonitrile with 0.1 M LiTFSI supporting electrolyte at a scan rate of 100 mV/s using a platinum disk working electrode, platinum mesh counter electrode and Ag/AgNO₃ (0.1 M TBAPF₆ acetonitrile) reference electrode.

References

- (1) Xie, Y.; Hamann, T. W. Fast Low-Spin Cobalt Complex Redox Shuttles for Dye-Sensitized Solar Cells. *J. Phys. Chem. Lett.* **2013**, *4* (2), 328–332.
- (2) Ahmad, S.; Bessho, T.; Kessler, F.; Baranoff, E.; Frey, J.; Yi, C.; Grätzel, M.; Nazeeruddin, M. K. A New Generation of Platinum and Iodine Free Efficient Dye-Sensitized Solar Cells. *Phys. Chem. Chem. Phys.* **2012**, *14* (30), 10631–10639.
- (3) Ren, X. F.; Alleyne, B. D.; Djurovich, P. I.; Adachi, C.; Tsyba, I.; Bau, R.; Thompson, M. E. Organometallic Complexes as Hole-Transporting Materials in Organic Light-Emitting Diodes. *Inorg. Chem.* **2004**, *43* (5), 1697–1707.
- (4) Connelly, N. G.; Geiger, W. E. Chemical Redox Agents for Organometallic Chemistry. *Chem. Rev.* **1996**, *96* (2), 877–910.
- (5) Xie, Y.; Baillargeon, J.; Hamann, T. W. Kinetics of Regeneration and Recombination Reactions in Dye-Sensitized Solar Cells Employing Cobalt Redox Shuttles. *J. Phys. Chem. C* **2015**, *119* (50), 28155–28166.
- (6) Marcus, R. A.; Sutin, N. Electron Transfers in Chemistry and Biology. *Biochim. Biophys. Acta.* **1985**, *811* (3), 265–322.